P2F.12 Simulations and Observations of Extreme Low-Level Updrafts in Hurricane Isabel

Daniel P. Stern[1*], David S. Nolan[1], and Sim D. Aberson[2]

[1]University of Miami/RSMAS

[2]NOAA/AOML/HRD

1. Introduction

Extreme low-level updrafts have previously been found to be ubiquitous features of intense tropical cyclones (Stern and Aberson 2006). Between 1997 and 2005, there were 77 dropsonde observations of extreme updrafts, which were defined to be any updraft stronger than the terminal fall speed of the sonde (~12-14 m/s). These "upsondes" were found almost exclusively in the eyewalls of major hurricanes, with 90% occurring within Category 4 and 5 storms. Herein, we demonstrate that high-resolution simulations of Hurricane Isabel produce similar features, and we investigate their cause.

There are numerous unanswered questions regarding low-level updrafts within tropical cyclones. These include their origin, spatial distribution, and relationship to larger scale structure and intensity. One of the more important questions is what can generate the forces required to produce a 15-25 m/s updraft at heights below 2.5 km. Some studies have concluded that eyewall updrafts are generally forced by local buoyancy (Braun 2002), while others (Zhang et al. 2000) have found the forcing to be due to dynamic pressure gradient forces. Few studies have examined low-level updrafts in particular, nor have they examined updrafts of "upsonde" magnitude.

Numerous studies have found the environmental vertical wind shear to be critical to the organization of updrafts within tropical cyclones (e.g. Corbosiero and Molinari 2003), with updrafts found preferentially downshear-left or left of shear, depending on the study. Other studies have also found motion-induced frictional asymmetry to be important, with updrafts located preferentially in the right-front quadrant relative to storm motion (Shapiro 1983). Again, most of these studies were not looking at low-level updrafts in particular. In Stern and Aberson, 44% of upsondes were found in the downshear-left quadrant, with another 38% upshear-left, and so shear was shown to be the dominant control on spatial distribution of extreme low-level updrafts. It is possible that these features are dynamically distinct from mid/upper-level updrafts, in which case their cause and the mechanisms which control their distribution may be different.

2. Model

We use WRF v2.2 to simulate Hurricane Isabel (2003) from 00Z 12th to 00Z 14th. The initial and lateral boundary conditions are provided by the GFDL 6-hourly analyses. There are 40 vertical levels, equally spaced in pressure. For the control simulation, we use 4 nested grids with horizontal resolutions of 12, 4, 1.33, and .444 km. The YSU PBL scheme is used, with a modified drag coefficient based on the results of Donelan et al. (2004). The WSM 5-class scheme was utilized for microphysics (Hong et al. 2004), while for radiation the RRTM longwave (Mlawer et al. 1997) and Goddard shortwave (Chou et al. 1998) schemes were used.

3. Intensity and Location

In Isabel on the 12th, extreme updrafts were observed by 6 dropsondes at 3 different times. The sondes first encountered the updrafts at various heights between 140 and 1500 m. The maximum vertical velocities were 13.1-17.3 m/s, and were located 21-28 km from the storm center. In Fig 1, the storm-relative loca-

*. Corresponding author address: Daniel P. Stern, RSMAS/MPO, 4600 Rickenbacker Causeway, Miami, FL, 33149; dstern@rsmas.miami.edu

tions of the upsondes are plotted along with all simulated updrafts exceeding 15 m/s from 15-23Z at 1 km height. During this time, the observed vertical shear was from the north at 12 kt, while the storm motion was towards the west at 4 kt. The simulated and observed updrafts are both located in the regions believed to be favored by shear, but not motion. The simulated updrafts are located 10-15 km radially outward from the observed, which is consistent with the simulated storm being too large by the same amount. Roughly 85% of all simulated 15 m/s updrafts below 2 km height occur in the left of shear semicircle (not shown).

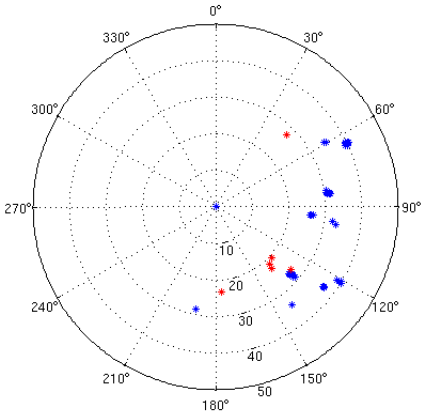

Fig 1: Storm-relative location of “upsondes” (red), and simulated updrafts exceeding 15 m/s from 15-23Z at a height of 1km (blue).

4. Evolution of an Updraft

An individual simulated updraft was tracked using 20-second output from 1800:00-1813:40. The maximum intensity was 27.5 m/s, at 1500 m height at 1806:20. Fig 2 shows a time series of the vertical velocity of the feature at various heights from 250-1500 m. Although already relatively strong at the initial time, the feature roughly doubled in intensity over a 6 minute period, and did so near-simultaneously throughout its depth. The largest accelerations apparently occur below 750 m. There are two phases of weakening: first a slow decay from 1806:20-1809:20, followed by a more rapid decay until 1813:40. The rapid weakening only occurs at and above 1 km, and at the lowest level (250 m), there is little or no weakening. The feature can be visually followed at the lowest few model levels for another 6 minutes (not shown), during which time the feature weakens to ~2 m/s and becomes indistinct at all levels. Figure 3 shows the vertical velocity as a function of height along the feature at 1 minute intervals, which illustrates the very shallow extent of these low-level updrafts. At no point does the feature extend above about 3.5 km height, and the height of maximum vertical velocity generally does not change with time until the feature weakens and the maximum drops to 750 m.

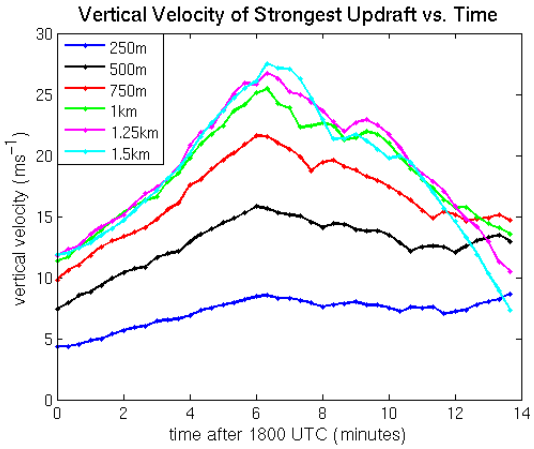

Fig 2: Time series of the vertical velocity of the tracked updraft.

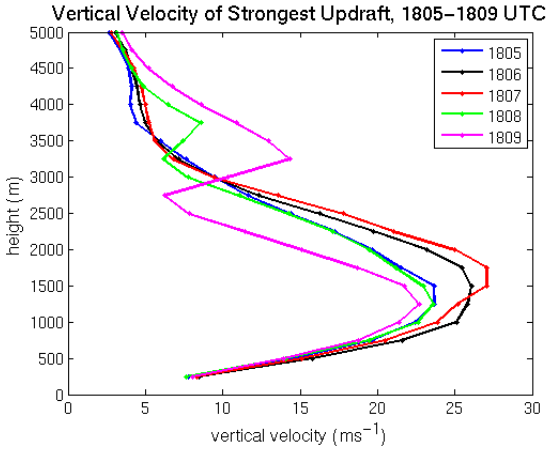

Fig 3: Vertical velocity vs. height at 1 minute intervals across time of peak intensity.

Figure 4 shows the radial and azimuthal slopes of the feature with height. The updraft tilts outward and

slightly cyclonically with height. At 30 km radius, the azimuthal tilt is ~250 m/km, while the outward tilt is 2-3 times larger. These slopes are much less than what would be expected from advection by the flow in which the feature is embedded, and so the quasi-steady structure must be dynamically maintained.

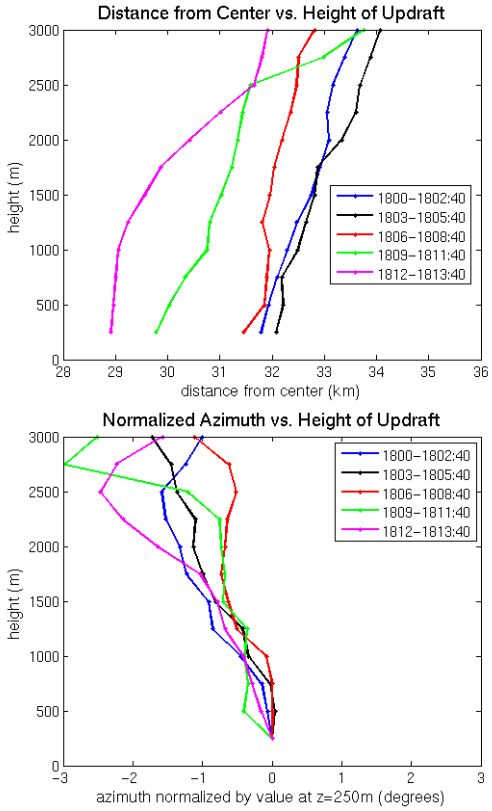

Fig 4: Distance from center vs. height (top), and azimuth vs. height (bottom). The azimuth at each height is subtracted from that at the lowest level. In both plots, each line represents a mean over a 3 minute period.

Figure 5 shows the storm-relative horizontal trajectory of the feature. As the feature translates ~110 degrees azimuthally in a 14 minute period, its tangential velocity is roughly 70 m/s. This may help explain the observed near equal preference of upsondes for the downshear-left and upshear-left quadrants; if this feature were to occur in a real storm, it would potentially be found in both quadrants. It is important to stress that this feature does not at all resemble the conceptual model of a rising bubble, and so the extreme updraft can be found at the same low-levels throughout its lifecycle.

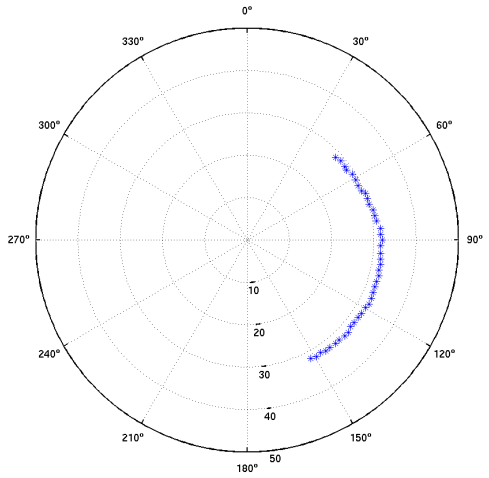

Fig 5: Storm-relative location of the tracked updraft at 20-second intervals, from 1800:00 to 1813:40.

5. Buoyancy?

We have not made quantitative calculations of buoyancy. However, we can definitively rule out buoyancy as the primary mechanism for parcel acceleration within this feature, using a simple estimate of the required forcing, following Eastin et al. (2003). If we assume a steady state feature with forcing (F) constant with height, then the rate of change of vertical velocity with height can be approximated as:

$$\frac{\partial w}{\partial z} = \frac{1}{w}F \tag{5.1}$$

which when integrated gives:

$$F = \frac{w^2}{2\Delta z} \tag{5.2}$$

Within this feature, we know that parcels must accelerate from roughly 0-15 m/s between the surface and 500 m height. So at a minimum, F must be .225 m/s^2 (it is possible that the parcels have experienced this change in velocity over a smaller depth). We can then estimate the thermal perturbation that would be required to produce this acceleration if buoyancy were the only force involved. If buoyancy (B) is given by:

$$B = g\frac{\theta'_v}{\overline{\theta_v}} \tag{5.3}$$

where g is gravity, and $\overline{\theta_v}$ is the reference virtual potential temperature (assumed to be 300 K), then the necessary perturbation virtual potential temperature θ'_v is 6.87 K. This is a very large value for low levels, and would be very noticeable from a cursory examination of a plot of the total virtual potential temperature. Such a plot is shown in Fig. 6, which consists of three stacked horizontal slices of θ_v in color, with vertical velocity contoured, in a 30x30 km domain centered on the feature. It is evident that such a large perturbation centered on the updraft does not exist, and any perturbations are an order of magnitude smaller. Furthermore, it is not even clear that the perturbations associated with the updrafts are positive, as the warmest air is actually located closer to the strongest downdrafts (not shown). Therefore, the forcing for this extreme updraft cannot be due to buoyancy, and must instead be due to dynamic nonhydrostatic pressure gradient forces.

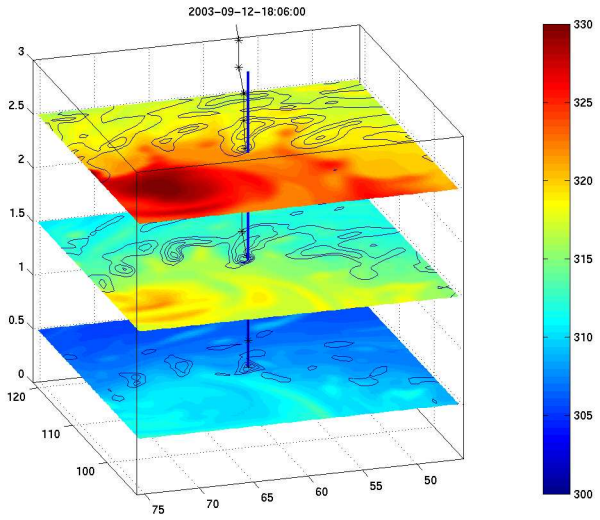

Fig 6: Virtual potential temperature (color), and vertical velocity (contoured every 5 m/s starting at 10 m/s). Domain is 30x30x3 km, and is centered on the maximum updraft at 750 m height. The view is looking outward from inside the eye towards the azimuth of the updraft.

6. Sensitivity to Resolution

To examine the sensitivity of updraft strength to resolution, we compare the simulation with 444 m resolution to one with 1.33 km resolution. To ensure that any differences are dynamically meaningful, the simulations are compared on the same 1.33 km grid. Shown in Fig. 7 is the mean over time of the maximum vertical velocity found at each height at hourly intervals from 15-23Z. It can be seen that below 2.5 km, the updrafts in the control simulation are 2-4 m/s stronger than those simulated at coarser resolution. In contrast, above 3.5 km, the magnitude of the strongest updrafts are practically identical. This is partly because the plot is of the strongest updraft at each level anywhere in the domain, and the strongest updraft at a given level is not necessarily connected to those above and below it. Indeed, the strongest updrafts above 3.5 km are almost never part of the same features as the strongest updrafts below. Apparently then, the extreme low-level updrafts are sensitive to these resolution changes, while the strong mid-level updrafts may not be. This in turn may be due to the smaller horizontal scale of the low-level updrafts versus the mid-level updrafts (not shown).

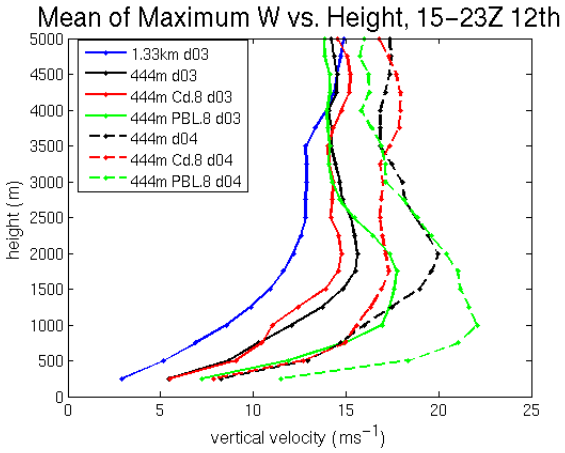

Fig 7: Mean of the domain maximum vertical velocity at each height, taken across hourly output from 15-23Z 12th. The resolution of the simulation is given as either 444 m or 1.33 km. “d03” refers to output on the 1.33 km grid, while “d04” refers to output on the 444 m grid. For the 444 m simulations, the data on the 1.33 km grid are interpolated from the 444 m grid.

7. Sensitivity to PBL Scheme

Also shown in Fig. 7 are the results of an additional pair of simulations performed with modifications to the PBL parameterization. Cd.8 refers to a simulation where the surface drag coefficient was reduced to 80% of its diagnosed value. PBL.8 refers to a simulation where the depth of the thermodynamic boundary layer was reduced to 80% of its diagnosed value. In Cd.8, the maximum updrafts are weakened by several m/s relative to the control simulation, while in PBL.8, the maximum updrafts are strengthened by several m/s. Additionally, in PBL.8 the height of the maximum updrafts lowers by 500-750 m. At this time, understanding of the reason for this sensitivity is limited, although the existence of the sensitivity strongly implies that these extreme updrafts are fundamentally tied to the boundary layer. A possible explanation of the decrease in maximum updraft with decreasing drag coefficient is that a decreased drag coefficient directly causes a reduction in frictional inflow. This will lead to a decrease in the vertical gradient of radial velocity, which appears to be a large source of the horizontal vorticity which is tilted into the vertical by the updraft. At all times, there is a strong local misovortex which is found just inward of the extreme updraft discussed in sections 4 and 5. The vertical vorticity and velocity fields are clearly tightly coupled, and so a reduction in the horizontal vorticity source could potentially be a cause of the reduced vertical velocities.

8. Summary and Discussion

We have shown that high-resolution simulations of Hurricane Isabel are able to produce very strong low-level updrafts, which compare favorably to observations, in magnitude and spatial distribution. By tracking an individual extreme updraft at high temporal resolution, we have begun to elucidate some aspects of the complex dynamics involved in producing these features. In particular, we have demonstrated that the forcing for the tracked updraft cannot be local buoyancy. This very likely holds true for other similar simulated features, which requires that dynamic nonhydrostatic pressure gradient forces must be the forcing. While this is more difficult to demonstrate in the observations, we should note that the same rough estimate of the thermal perturbations required to generate such updrafts applies equally well. 15 m/s updrafts have been observed at and below 500 m height, and a 13.1 m/s updraft was observed at 140 m in Isabel on the 12th. Such an updraft would require a ~19 K temperature perturbation if produced by buoyancy! Therefore, the observed upsondes are also very unlikely to be driven by buoyancy.

It appears that some of the strongest simulated horizontal winds are found slightly upstream, radially outward, and below the extreme updrafts (not shown). This is consistent with the production of vertical vorticity by the updraft in a region of very strong radial shear of the mean tangential winds. The extreme low-level updrafts are potentially an important mechanism by which the strongest horizontal windspeeds in tropical cyclones are produced. This is also consistent with the strong overlap between the observed upsondes and the set of all sondes in which 90 m/s horizontal winds are found (Aberson and Stern 2006). This may have implications for the mechanism by which extreme wind damage is produced in landfalling major hurricanes.

9. References

Aberson, S. D. and D. P. Stern, 2006: Extreme horizontal winds measured by dropwindsondes in hurricanes. *Preprints, 27th AMS Conference on Hurricanes and Tropical Meteorology,* Monterey, CA, April 2006.

Braun, S. A., 2002: A cloud-resolving simulation of Hurricane Bob (1991): Storm structure and eyewall buoyancy. *Mon. Wea. Rev.*, **130**, 1573-1592.

Chou, M.-D., M. J. Suarez, C.-H. Ho, M. M.-H. Yan, and K.-T. Lee, 1998: Parameterizations for cloud overlapping and shortwave single-scattering properties for use in general circulation and cloud ensemble models. *J. Climate*, **11**, 202-214.

Corbosiero, K. L. and J. Molinari, 2003: The relationship between storm motion, vertical wind shear, and convective asymmetries in tropical cyclones. *J. Atmos. Sci.*, **60**, 366-376.

Donelan, M. A. et al., 2004: On the limiting aerodynamic roughness of the ocean in very strong winds. *GRL*, **31**, L18306.

Eastin, M. D., W. M. Gray, and P. G. Black, 2005: Buoyancy of convective vertical motions in the inner core of intense hurricanes. Part I: General statistics. *Mon. Wea. Rev.*, **133**, 188-208.

Hong, S.-Y., J. Dudhia, and S.-H. Chen, 2004: A revised approach to ice microphysical processes for the bulk parameterization of clouds and precipitation. *Mon. Wea. Rev.*, **132**, 103-120.

Mlawer, E. J., S. J. Taubman, P. D. Brown, M. J. Iacono, and S. A. Clough, 1997: Radiative transfer for inhomogeneous atmospheres: RRTM, a validated correlated-k model for the longwave. *JGR*, **102**(D14), 16663-16682.

Shapiro, L. J., 1983: The asymmetric boundary layer flow under a translating hurricane. *J. Atmos. Sci.*, **40**, 1984-1998.

Stern, D. P. and S. D. Aberson, 2006: Extreme vertical winds measured by dropwindsondes in hurricanes. *Preprints, 27th AMS Conference on Hurricanes and Tropical Meteorology*, Monterey, CA, April 2006.

Zhang, D.-L., Y. Liu, and M. K. Yau, 2000: A multiscale numerical study of Hurricane Andrew (1992). Part III: Dynamically induced vertical motion. *Mon. Wea. Rev.*, **128**, 3772-3788.